ELSEVIER

Journal of Power Sources 69 (1997) 145–156

JOURNAL OF POWER SOURCES

Extraction of lithium from spinel phases of the system $Li_{1+x}Mn_{2-x}O_{4-\delta}$

P. Endres [a], A. Ott [a], S. Kemmler-Sack [a,*], A. Jäger [a], H.A. Mayer [a], H.-W. Praas [b], K. Brandt [b]

[a] *Institut für Anorganische Chemie der Universität, Auf der Morgenstelle 18, 72076 Tübingen, Germany*

[b] *VARTA Batterie AG, Research and Development Center, Gundelhardtstraße 72, 65779 Kelkheim, Germany*

Received 17 October 1996; revised 4 February 1997

Abstract

The process of chemical lithium extraction from the spinel phase $Li_{1+x}Mn_{2-x}O_{4-\delta}$ was studied for $0 \le x \le 0.33$ in acidic medium (H_2SO_4/H_2O) and Br_2/CH_3CN as proton-free extraction liquid. From a comparison of the quantitative results of chemical delithiation with the electrochemical performance there follows a subdivision into three regions. In region I ($0 \le x \le 0.05$) the extraction products are multiphase due to a pronounced lattice instability. The electrochemical performance is unsatisfying. The best materials for cathodes in rechargeable Li-ion batteries are situated in region II ($0.05 \le x \le 0.2$). All extraction products are single phase due to an improved lattice stability. In region III ($0.2 \le x \le 0.33$) the capacity is too low for practical applications. All materials are oxygen deficient and show a strong tendency for an ion exchange $Li^+ \leftrightarrow H^+$ in protonic solvents. In acidic media, the Hunter mechanism is obeyed for $x = 0$. With increasing x this model is suppressed in favour of a $Li^+ \leftrightarrow H^+$ exchange. © 1997 Elsevier Science S.A.

Keywords: Spinel; Lithium manganese oxides

1. Introduction

Active materials which can be applied as cathodes in rechargeable lithium-ion batteries of high voltage (about 4 V) are the layered oxides $LiCoO_2$ and $LiNiO_2$ (space group $R\bar{3}m$ [1]) and the cubic spinel $LiMn_2O_4$ ($Fd\bar{3}m$ [2–6]). From the point of view of starting materials, price, and toxicity, the $LiMn_2O_4$ spinel has a considerable advantage. However, its rechargeable capacity and cycleability in the 4 V region are inferior to that of the layered oxides. Several attempts to improve the electrochemical properties of $LiMn_2O_4$ in the 4 V region have been reported. The most effective candidate is low-valent cation doping to 16*d* sites (denoted by square brackets), $Li[M_yMn_{2-y}]O_4$ for M^{y+} with $y < 3.5$, because it reduces the content of the Jahn–Teller ion Mn^{3+} and stabilizes the cubic spinel structure [7]. Monovalent Li doping seems to be best due to the larger charge difference relative to Mn. Thus, a small fraction of dopant is effective and lattice disturbances are minimized which may result in localization of the charge carriers Li^+ and e^-. A second advantage of Li doping is the prevention of foreign, non Li ions from occupying the tetrahedral 8*a* sites which will hamper the migration of Li between the tetrahedral and octahedral sites, resulting in a decrease of rechargeable capacity.

Recently, Li-rich spinels of type $Li[Li_xMn_{2-x}]O_4$ [4,8] were synthesized. Further investigations reveal a slight oxygen deficiency of the spinel system: $Li_{1+x}Mn_{2-x}O_{4-\delta}$ [5,6]. In addition, it was shown that the rechargeable capacity in the 4 V region is strongly dependent on the Li/Mn ratio [4,6]. Moreover, a detailed study of the influence of x on the electrochemical performance reveals that for small values of x the rechargeable capacity is higher than for $LiMn_2O_4$ [6]. Interestingly, for x around 0.05 the theoretical capacity (calculated for the system $Li[Li_xMn_{2-x}]O_4$) is obtained. For example Fig. 1 shows the dependence of the first charge capacity (3.3–4.3 V) of the spinel phase $Li_{1+x}Mn_{2-x}O_{4-\delta}$ ($0 \le x \le 0.33$). Its electrochemical performance can be roughly divided in three regions: in region I ($x \le 0.05$) the experimental capacity is inferior to the calculated value; in region II ($0.05 \le x \le 0.2$) rechargeable capacity and theory are practically in agreement; whereas in region III ($0.2 \le x \le 0.33$) the electrochemical performance is better than expected for spinels without deficiency of oxygen ($\delta = 0$).

The observed dependence of the capacity on x does not agree with the generally accepted correlation between Mn^{3+} content and quantity of extracted Li, first reported by Hunter (Hunter mechanism) for Li extraction from acid media for

* Corresponding author: Tel.: +49 (7071) 297 24 39; Fax: +49 (7071) 29 69 18; e-mail: ks@uni-tuebingen.de or kemmler-sack@uni-tuebingen.de

PII S0378-7753(97)02604-9

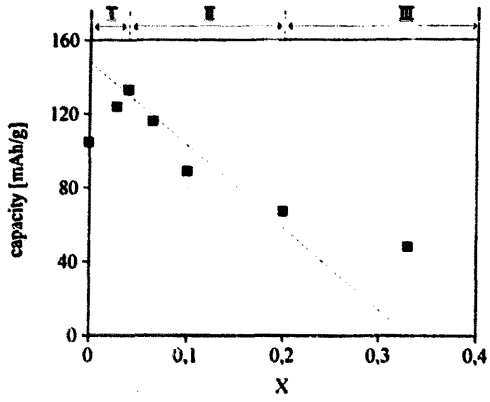

Fig. 1. The first charge capacity (3.3–4.3 V) of the spinel phase $Li_{1+x}Mn_{2-x}O_{4-\delta}$. The broken line is the theoretical capacity for $\delta = 0$.

the reaction between $LiMn_2O_4$ and the protons of the solvent [9]. A more extended description of the Hunter mechanism is given later on by Goodenough et al. [10]

$$2LiMn_2O_4 + 4H^+ \rightarrow 3MnO_2 + Mn^{2+} + 2Li + 3H_2O \quad (1)$$

According to these considerations an electrochemical Li extraction from $LiMn_2O_4$ is accompanied by an oxidation of Mn^{3+} to Mn^{4+}. Thus, the extent of extracted Li correlates with the Mn^{3+} content. For $x = 0$ the Mn^{3+}-free endproduct has the composition $\square Mn_2^{4+}O_4$ (λ-MnO_2), whereas for the Li-rich endmember $Li_{4/3}Mn_{5/3}^{4+}O_4$ with $x = 0.33$ no Li extraction is expected. However, the experimental data in Fig. 1 indicate that the supposed correlation is only valid in region II.

To get a better insight into the process of Li extraction, the aim of the present investigation was to study the correlation between the amount of extracted Li and the Mn^{3+} content quantitatively under action of different extraction media in the entire spinel phase $Li_{1+x}Mn_{2-x}O_{4-\delta}$. The validity of the Hunter mechanism is investigated for several analytically controlled H^+ concentrations by applying various mixtures of H_2SO_4/H_2O. For comparison we studied the mechanism of Li extraction in Br_2/CH_3CN as a proton-free extraction medium. Up to now the properties of chemical Li extraction were studied only for the 1:2 spinel $LiMn_2O_4$ ($x = 0$) by several authors [8–15].

2. Experimental

For the synthesis of several members from the spinel phase $Li_{1+x}Mn_{2-x}O_{4-\delta}$ with $x = 0; 0.05; 0.1; 0.15; 0.20; 0.25; 0.30; 0.33$ and $0 \leq \delta \leq 0.2$, the starting materials β-MnO_2 (Selectipur; Merck) and $LiOH \cdot H_2O$ (Alfa Ventron) were thoroughly mixed in an agate mortar and heated in corundum boats (Degussit Al 23) in air at temperatures between 400 and 850 °C. The correlation between the reaction temperature and the parameter x is indicated in Fig. 2. The total reaction time of 20 h was interrupted after 4 h for regrinding and X-ray analysis (XRD; Philips powder diffractometer, Ni filtered

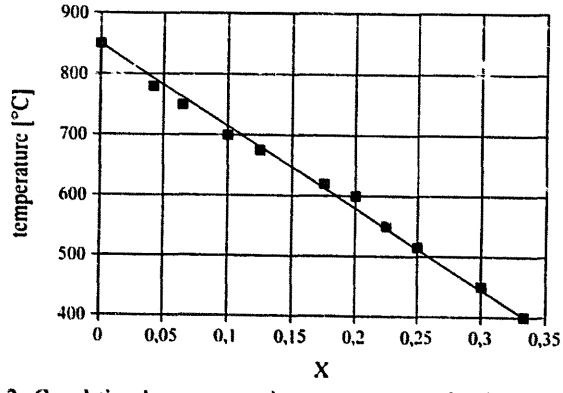

Fig. 2. Correlation between reaction temperature and x in the system $Li_{1+x}Mn_{2-x}O_{4-\delta}$.

Cu Kα radiation, Au standard). All materials were quenched to room temperature (RT) from their reaction temperature.

Acid Li extraction from 4 g of spinel was performed with 300 ml of stirred mixtures from H_2SO_4/H_2O with different ratios between $(H^+:Li[Li_xMn_{2-x}]O_{4-\delta}) = 0.25; 0.5; 1.0; 2.0; 3.0; 4.0$. During the reaction the pH value was followed potentiometrically. After about 3 days a constant value was obtained, indicating the end of the reaction. The quantity of effectively consumed H^+ was calculated from the difference between starting and the end concentration of H^+. In addition, corrections for the second dissociation step of H_2SO_4 ($HSO_4^- + H_2O \rightarrow SO_4^{2-} + H_3O^+$; $pK_s = 1.92$) were applied. The residue was dried in vacuum over P_4O_{10}. The content of Li and Mn was determined in both residue and the extraction liquid by atomic absorption spectroscopy (AAS) or complexometric titration, respectively. The Li extraction with Br_2/CH_3CN was performed in Ar atmosphere with a stirred solution of 100 ml CH_3CN (Fluka, puriss.) and a fivefold excess of Br_2 during 2 days at RT. The Li and Mn content was determined in the residue, additionally, the Li content of the solvent was measured. The average oxidation state of manganese was studied by redox titration (Metrohm Titroprocessor 686).

The IR spectra were measured with a Perkin-Elmer spectrometer (FT-IR 1600). The solid-state nuclear magnetic resonance (NMR) data were recorded on a Bruker ASX300 (7.05T) spectrometer in a commercial 4 mm rotor with spinning speeds from 5–12 kHz. Frequencies and standards: ^7Li, 116.70 MHz (1.0 M LiCl solution in H_2O); ^1H, 300.13 MHz (TMS).

3. Results and discussion

3.1. Li extraction from the system $Li_{1+x}Mn_{2-x}O_{4-\delta}$ by Br_2/CH_3CN

3.1.1. Chemical composition and crystal structure

During the Li extraction with Br_2 in proton-free solvents oxidation of Mn^{3+} to Mn^{4+} ($Mn^{3+} + 1/2Br_2 \rightarrow Mn^{4+} + Br^-$) takes place according to the general relation

$$Li[Li_xMn_{1-3x}^{3+}Mn_{1+2x}^{4+}]O_{4-\delta}+y/2Br_2 \rightarrow Li_{1-y}[Li_xMn_{1-3x-y}^{3+}Mn_{1+2x+y}^{4+}]O_{4-\delta} + yLiBr \quad (2)$$

with y as parameter of the extracted quantity of Li from the tetrahedral 8*a* positions. (Note that in contrast with the case of the Hunter mechanism for proton-containing solvents, in the present case the extraction of Li is not accompanied by a partial dissolution of the spinel phase.) Due to the simple oxidation of the host matrix $[Li_xMn_{1-3x}^{3+}Mn_{1+2x}^{4+}]O_{4-\delta}$ during Li extraction the de-intercalation mechanism in proton-free solvents is assumed to agree with the case of electrochemical Li extraction.

According to our analytical studies (Table 1; comprehensive data are indicated Ref. [16]) of residue and extraction liquid no dissolution of the host matrix takes place because the Mn content of the residue remains constant. The quantity of the extracted Li is around 0.3 Li per formula unit within the entire spinel phase $Li_{1+x}Mn_{2-x}O_{4-\delta}$ (sample nos. 1–8 in Table 1). The average oxidation state of Mn, Ox_{Mn}, remains always below the border-line case of +4.00 and even the residue of the Li-rich spinel with the lowest Mn^{3+} content (sample no. 8) still contains about 30% of the original Mn^{3+} fraction. Note that the extracted Li fraction is lower than the nominal Mn^{3+} content.)

In another series of experiments (sample nos. 8–10, Table 1) we have shown that for a fixed Li:Mn ratio but with decreasing Mn^{3+} content (increasing average oxidation state of Mn in the starting product), a clear correlation between the extracted Li fraction and the Mn^{3+} content is present. Correspondingly, Ox_{Mn} of the extraction product increases but never reaches the ideal value of +4.00. This finding indicates, that lattice vacancies are always present. The composition of the extraction products is given in Table 1.

XRD diagrams of the starting materials show the typical diffraction pattern of single phase cubic spinels [5,6]. The lattice constants are indicated in Table 1. XRD diagrams of the corresponding extraction residues are summarized in Fig. 3. Note that only Li-rich spinels with $0.1 \leq x \leq 0.33$ yield single phase materials with the typical diffraction pattern of a cubic spinel. Due to the small scattering power of Li, the XRD diagram mainly correlates with the Mn and O containing host matrix. However, for $x=0$ and 0.05 no single phase extraction products were obtained.

From the appearance of three peaks in the region of the (111) reflection of a cubic spinel lattice, it follows that the multiphase extraction product contains in addition to the cubic main phase with the most intense central peak two spinel related smaller fractions of byproducts. (Note that in the entire series, the XRD diagrams of the residue do not vary after grinding, as was observed in some spinel phases with noble metals [18]). As was observed by Ohzuku et al. [19] electrochemically prepared spinels with a composition of $Li_{0.6}Mn_2O_4$ are multiphase and consists of two spinel phases.

For $x=0$ and $x=0.05$ the lattice constant of the main spinel phase are identical (Table 1). Furthermore, they agree with the value for single phase spinel with $x=0.1$. From this coincidence the atomic arrangement in these three spinel phases is deduced to be identical. The instability of the crystal structure versus Li extraction for $x=0$ and 0.05 is due to the relatively expanded spinel framework and a comparably large volume decrease of around 3% between extraction product and starting material. A little smaller spinel framework will provide a more reversible structure for Li exchange. Espe-

Table 1
Chemical composition, lattice constants, average oxidation state of Mn(Ox_{Mn}) and decrease of the unit cell volume (ΔV) for spinel phases of the system $Li_{1+x-y}Mn_{2-x}O_{4-\delta}$ before ($y=0$) and after extraction with Br_2/CH_3CN

Sample no.	Composition of starting product	Composition of extraction product [a]	Lattice constant (Å; ±0.003)		Ox_{Mn}			ΔV (%)
			Starting product	Extraction product	Starting product	Extraction product, calc.	Extraction product, exp.	
1	$Li[Mn_2]O_4$	"$Li_{0.60}[Mn_2]O_4$" [b]	8.247	8.165 [c]	+3.50	+3.70	+3.71	2.95 [c]
2	$Li[Li_{0.05}Mn_{1.95}]O_4$	"$Li_{0.60}[Li_{0.05}Mn_{1.95}]O_4$" [b]	8.242	8.165 [c]	+3.56	+3.77	+3.78	2.77 [c]
3	$Li[Li_{0.1}Mn_{1.9}]O_{3.98}$	$Li_{0.75}[Li_{0.1}Mn_{1.9}]O_{3.98}$	8.233	8.166	+3.61	+3.74	+3.75	2.42
4	$Li[Li_{0.15}Mn_{1.85}]O_{3.95}$	$Li_{0.60}[Li_{0.15}Mn_{1.85}]O_{3.95}$	8.218	8.135	+3.65	+3.86	+3.84	3.00
5	$Li[Li_{0.2}Mn_{1.8}]O_{3.93}$	$Li_{0.74}[Li_{0.2}Mn_{1.8}]O_{3.93}$	8.197	8.150	+3.70	+3.84	+3.81	1.71
6	$Li[Li_{0.25}Mn_{1.75}]O_{3.91}$	$Li_{0.75}[Li_{0.25}Mn_{1.75}]O_{3.91}$	8.180	8.141	+3.75	+3.87	+3.81	1.42
7	$Li[Li_{0.3}Mn_{1.7}]O_{3.86}$	$Li_{0.77}[Li_{0.3}Mn_{1.7}]O_{3.86}$	8.167	8.137	+3.78	+3.89	+3.88	1.10
8	$Li[Li_{1/3}Mn_{5/3}]O_{3.81}$	$Li_{0.72}[Li_{1/3}Mn_{5/3}]O_{3.81}$	8.165	8.135	+3.76	+3.93	+3.88	1.11
9	$Li[Li_{1/3}Mn_{5/3}]O_{3.87}^{d}$	$Li_{0.81}[Li_{1/3}Mn_{5/3}]O_{3.87}$	8.157	8.137	+3.84	+3.95	+3.87	0.73
10	$Li[Li_{1/3}Mn_{5/3}]O_{3.92}^{e}$	$Li_{0.87}[Li_{1/3}Mn_{5/3}]O_{3.92}$	8.143	8.128	+3.90	+3.98	+3.94	0.55

[a] Calculated from the analytical data with a fixed Li:Mn ratio in 16*d*.
[b] Multiphase.
[c] Main phase.
[d] Prepared by additional long-term annealing in flowing oxygen (400 °C/1300 h).
[e] Prepared by additional long-term annealing in flowing oxygen (400 °C/3000 h).

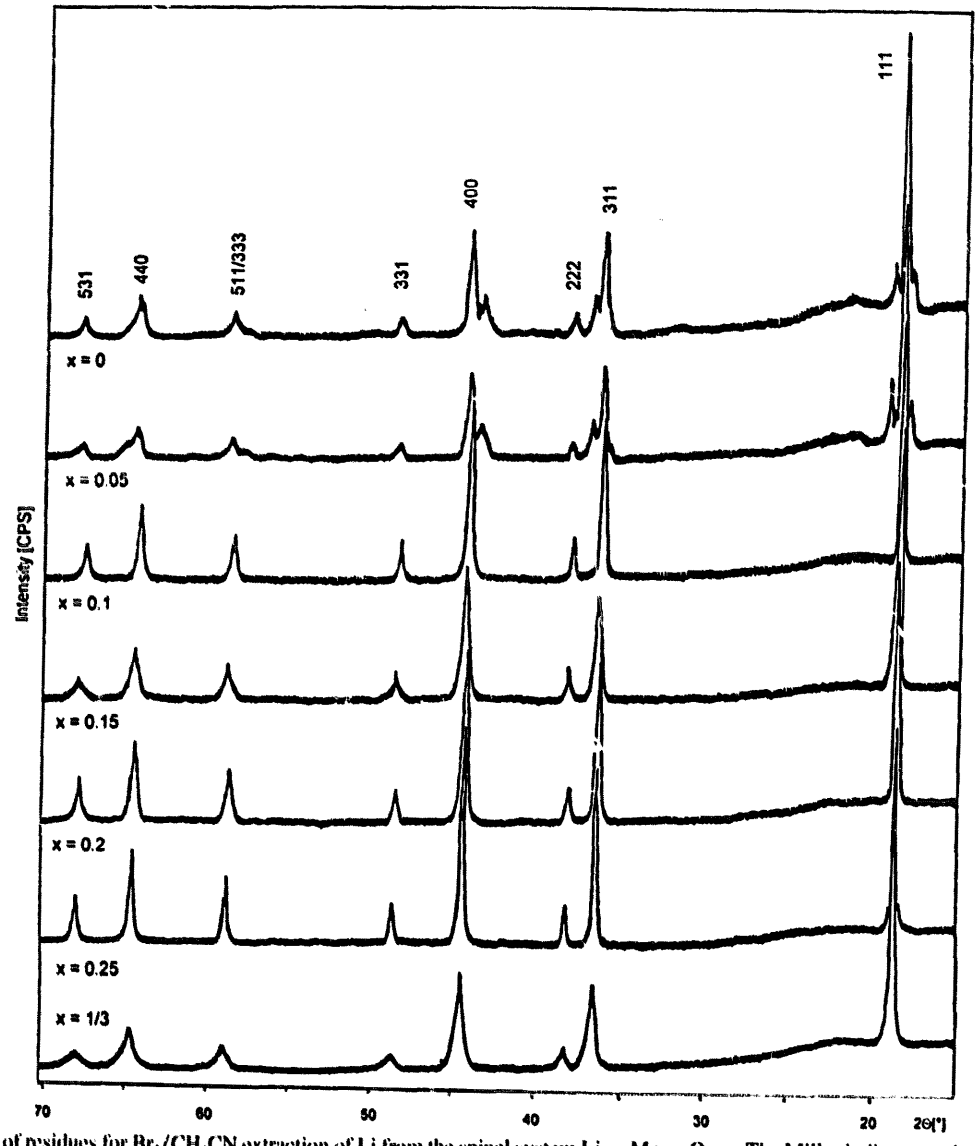

Fig. 3. XRD diagrams of residues for Br_2/CH_3CN extraction of Li from the spinel system $Li_{1+x}Mn_{2-x}O_4$. The Miller indices are given for each Bragg peak with reference to the setting of the cubic spinel unit cell ($Fd3m$).

cially, the high volume drop of about 7.5% for acidic delithiation (cf. Section 3.2.3) and electrochemical Li extraction from $Li[Mn_2]O_4$ is one reason for the pronounced fading of the rechargeable capacity [6,19,20].

Experiments of electrochemical Li extraction from $LiMn_2O_4$ ($x=0$) show a clear correlation between lattice constant and Li content [19,20]. The presence of two pairs of redox peaks at about 4.00 and 4.10 V (oxidation potential versus Li/Li^+) for $x=0$ and about 4.05 and 4.16 V ($x=0.04$ and $x=0.1$) in the cyclic voltammogram suggests that Li ions are extracted and inserted into the spinel phase by a two-step process. These two peaks may originate from the fact that Li ions are firstly removed from half of the tetrahedral 8*a* sites with Li–Li interaction, and then Li ions are removed from the other 8*a* sites without nearest neighbour Li–Li interaction [20]. From the crystallographic point of view this model is explained by a splitting of the original sublattice of diamond type Li in 8*a* into two face-centered-cubic lattices shifted one against the other by (1/4, 1/4, 1/4). The decrease of the spinel lattice constant with increasing degree of extraction proceeds stepwise due to an ordering of Li within the tetrahedral 8*a* positions [19–21]. The observed difference in redox potential depends on the difference in energy of the two sets of tetrahedral Li ions. An extraction of the first set of Li ions affords less energy than for the second set due to the stronger attractive forces as result of the increasing Mn^{4+} content. Whereas the removal of Li for $x=0$ proceeds in a two-step process, for $x=0.04$ and $x=0.1$ as second possibility a simultaneous removal of Li is observed in the cyclic voltammograms [20].

The redox potential of Br_2/Br^- in CH_3CN versus Li^+/Li is 4.1 V [22]. Accordingly, by application of Br_2/CH_3CN as extraction medium, the first set of Li ions with the lower redox potential of about 4.00 and 4.05 V should be removed, whereas an extraction from the deeper Li positions with its extraction peak around 4.10 and 4.16 V is expected to be more difficult. Indeed, the observed extraction level is relatively low and remains below the borderline value of $y=0.5$

even for $x = 0$. The lattice constant of the present main extraction product with $x = 0$ is similar to that of an electrochemical extraction product with identical Li content (e.g. [20]). (Note that no admixture of a fully extracted spinel phase with a lattice constant around 8.07 Å is observed.) Thus, according to its redox potential, Br_2/CH_3CN is only able to extract Li from the first set of more loosely bonded Li ions. An identical behaviour is observed in all Li-rich extraction products ($x \geq 0.1$). With decreasing Mn content in 16*d* the lattice constant of the extraction products decreases but never reaches values below about 8.1 Å, considered typical for the presence of the second extraction step. In agreement with the improved rigidity of the starting spinel framework, the contraction of the unit cell decreases during Li extraction (cf. ΔV in Table 1).

Note that Li/Mn spinels without Mn^{3+} are not accessible for an Li extraction by Br_2/CH_3CN. We studied this reaction for the well-known spinel $LiCr^{3+}Mn^{4+}O_4$ [16,17] under identical conditions as for $LiMn_2O_4$, but no Li extraction was observed. However, the absence of Mn^{3+} is not the only difference between $LiMn_2O_4$ and $LiCrMnO_4$. In addition, the apparent valency of Li is much higher in $LiCrMnO_4$ than in $LiMn_2O_4$ (cf. Section 3.1.2).

3.1.2. ^{7}Li–MAS–NMR spectra

The ^{7}Li–NMR spectrum of $LiMn_2O_4$ is shown, together with the spectrum of $LiCrMnO_4$, in Fig. 4. For both compounds the NMR spectrum exhibits a single line spaced by spinning side bands. The Knight shift is situated around 540 ppm ($LiMn_2O_4$) and 5 ppm ($LiCrMnO_4$), respectively. The quantity of the Knight shift is proportional to the electron density of the nucleus, when the spectrum is measured at a constant temperature [23]. The density of states was estimated from the Knight shift as in case of lithium metal and the apparent valences were obtained from the density of states. The quantity of the Knight shift of $LiMn_2O_4$ is in agreement with the data from the literature [23,24] and much larger than that of Li metal (256 ppm). The calculated electron density of ≈0.9 (electron density of Li in the compound/electron density of Li in atomic state) of $LiMn_2O_4$ is higher than for Li metal (0.44 [25]). This means that an average 90% of 2s electron is located at the lithium nucleus and Li exists in an almost atomic state. Thus, the charge distribution in $LiMn_2O_4$ can be described by the borderline case $Li_0Mn_2^{4+}O_4$. Note that the Li–Li distance in 8*a* is 3.57 Å. This distance is much larger than in Li metal with 3.04 Å. Furthermore, due to its relatively low electrical conductivity [26] $LiMn_2O_4$ is a semiconductor. However, as a consequence of the localization of about 90% of the 2s electron at the Li nucleus, the Mn^{3+} content in $LiMn_2O_4$ is considerably reduced. This finding easily explains the absence of a Jahn–Teller distortion. Moreover, the mechanism of Li extraction cannot be described via a combined oxidation of Mn^{3+} according to the relation $Mn^{3+} + Li^+ \leftrightarrow Mn^{4+} + Li^0$.

On the other hand, by substitution of one Mn in $LiMn_2O_4$ with Cr^{3+}, an ion with a fixed valence, the resulting spinel $LiCrMnO_4$ does not show any Knight shift. In this case lithium exists in completely ionic state with an apparent valence of +1.0 and the charge distribution is $Li^+Cr^{3+}Mn^{4+}O_4$.

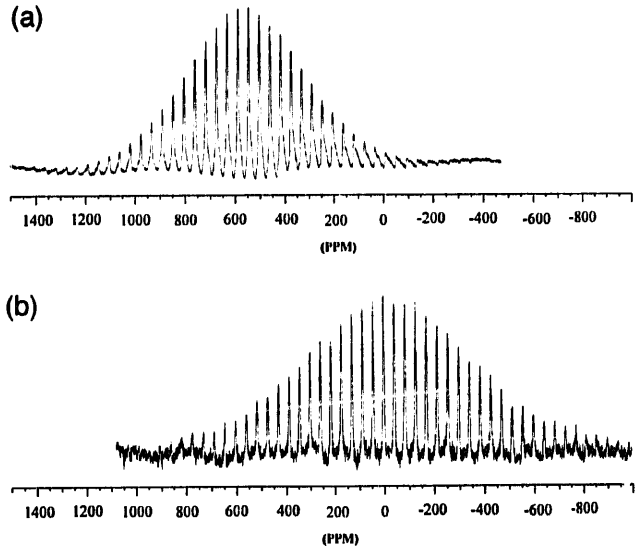

Fig. 4. ^{7}Li-MAS-NMR spectra of (a) $LiMn_2O_4$ and (b) $LiCrMnO_4$.

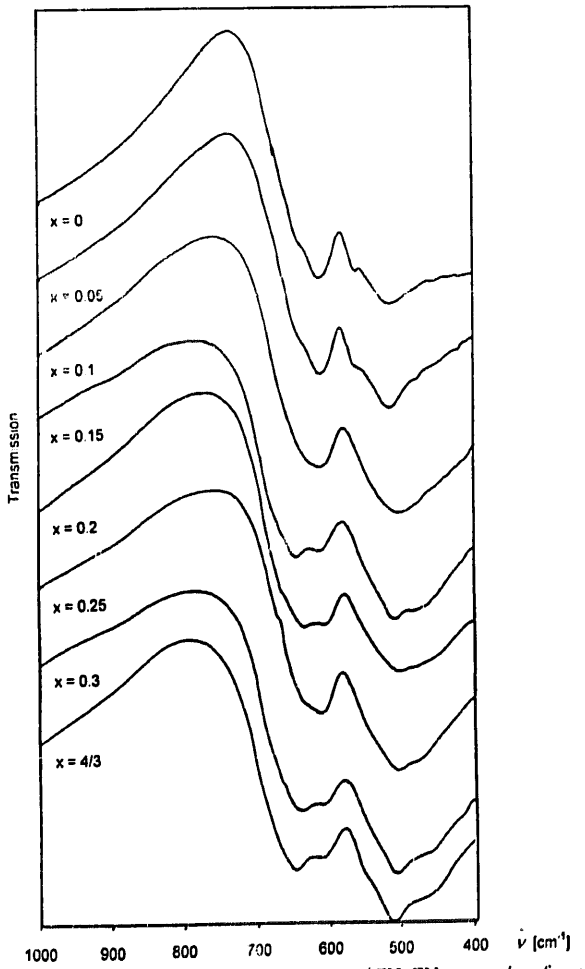

Fig. 5. IR spectra of some residues for Br_2/CH_3CN extraction from the spinel system $Li_{1+x}Mn_{2-x}O_{4-\delta}$. For clarity the spectra are shifted along the y-axis.

3.1.3. FT-IR spectra

The FT-IR spectra of several extraction products are shown in Fig. 5. In agreement with earlier observations [5,6] the spectra are uniformely characterized by two intense groups of vibrations around 650 and 550 cm^{-1}, assigned according to Tarte et al. [27–29] as ν_1 and ν_2/ν_3 of the spinel lattice. Compared with the FT-IR spectra of the corresponding starting materials no shift of the centre of gravity for each group of vibrations is observed. The extraction products show only some slightly more pronounced shoulders at the higher and lower energetic side of each central peak.

3.2. Li extraction from the system $Li_{1+x}Mn_{2-x}O_{4-\delta}$ by H_2SO_4/H_2O

3.2.1. Chemical composition

Li extraction from several members of the spinel phase $Li_{1+x}Mn_{2-x}O_{4-\delta}$ was performed with different molar ratios of H^+:$Li_{1+x}Mn_{2-x}O_{4-\delta}$ as indicated in Table 2 (for (H^+:$Li_{1+x}Mn_{2-x}O_{4-\delta}$) = 2.0–4.0 the results are identical within the limit of the experimental error). The content of Li and Mn was determined in both the residue and the extraction liquid. The sum of both values is in excellent agreement with the Li and Mn percentage of the corresponding starting material. The Li:Mn:O ratio of the extraction residue is indicated in Table 2. By validity of the Hunter mechanism (cf. Section 1) a linear correlation between the concentration of H^+ and the quantity of the extracted Li and Mn is predicted. Figs. 6 and 7 show the experimentally observed concentration dependence of Li or Mn versus the consumed H^+ concentration of the extraction medium together with the calculated correlation for the Hunter mechanism (a comprehensive data set is given in Ref. [30]). Note that in both cases no validity of the Hunter mechanism is found within the entire spinel phase $Li_{1+x-y}Mn_{2-x}O_{4-\delta}$). The deviations from the calculated linear dependence increase with increasing x, indicating an intensifying violation of the Hunter mechanism for Li-rich spinels. Moreover, in the Li-rich region the quantity of extracted Li exceeds the expected values, whereas the Mn concentration in the solvent is reduced. Accordingly, the postulated correlation between the extracted Li and Mn is lost for the Li-rich spinels.

From a comparison of the experimental overall oxidation state of Mn (Ox_{Mn}) for the extraction residues with the calculated values for the analytically determined Li and Mn content (cf. Li:Mn:O ratio of the forth column in Table 2), there follows an excellent agreement for the values with $x = 0$. In this case Ox_{Mn} increases with the degree of Li extraction and finally reaches a value near +4.00 in the highly extracted material. In cases with larger Li content ($0.05 < x < 0.3$) the same trend is present. However, the calculated values of the highly extracted materials (e.g. samples nos. 2d, 3d, 4d, 5d, 6d or 7d) are situated above +4.00. Moreover, the deviations increase with increasing x. This finding may be interpreted by an increasing incorporation of Mn with a valency higher than +4.0. However, the experimental values are in contradiction and never exceed the borderline case of +4.00. Thus, the experimental Ox_{Mn} values disagree with the observed Li:Mn:O ratio.

This deviation is explained by making a balance between the applied and consumed H^+ ions. Due to the consumption of less H^+ for the Li extraction than postulated by the Hunter mechanism (Fig. 6), some Li must be extracted by an ion exchange $Li^+ \leftrightarrow H^+$ as a second extraction mechanism. We determined the content of the ion exchanged H^+ in the residue via the difference between the consumed H^+ ions and the H^+ amount corresponding to the really extracted quantity of Li^+ according to the Hunter model. These values are indicated as H^+ content from H^+ balance in the eighth column

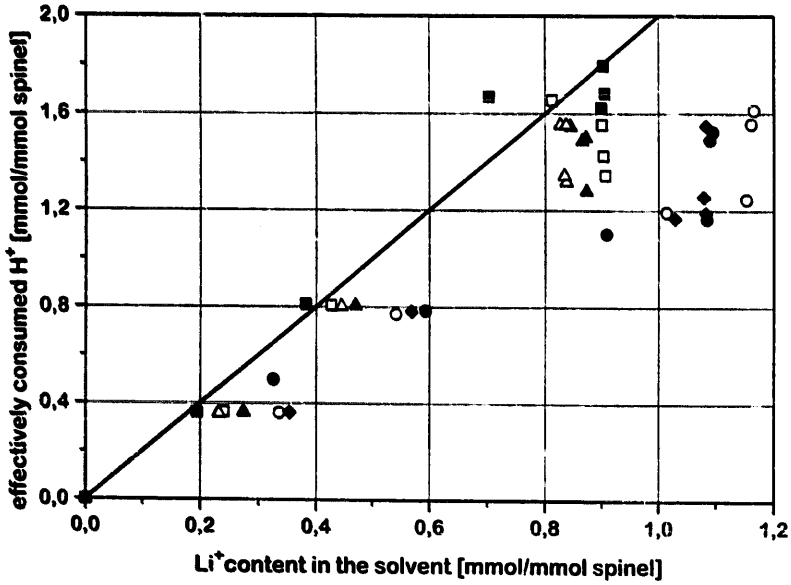

Fig. 6. Dependence of the effectively consumed H^+ vs. Li^+ content in the solvent for H_2SO_4/H_2O extraction of one mmole for several members from the spinel system $Li_{1-y}[Li_yMn_{2-x}]O_{4-\delta}$ for: (■) $x = 0$; (□) $x = 0.05$; (△) $x = 0.1$; (▲) $x = 0.15$; (●) $x = 0.2$; (○) $x = 0.25$, and (◆) $x = 0.3$. The solid line is the calculated correlation by validity of the Hunter mechanism.

Table 2
H^+:$Li_{1+x}Mn_{2-x}O_{4-\delta}$ ratio in the extraction process, analytically determined Li:Mn:O ratio, lattice constant [b], average oxidation state of Mn (Ox_{Mn}) and H^+ content for H_2SO_4/H_2O extraction products of the system $Li_{1+x-y}Mn_{2-x}O_{4-\delta}$

Sample no.	x	H^+:$Li_{1+x}Mn_{2-x}O_{4-\delta}$	Li:Mn:O ratio [a]	Lattice constant (Å) [b]	Ox_{Mn}		H^+ content H^+ balance [f]	ΔOx_{Mn} [g]
					calculated [c]	experimental		
1a	0	0.25	"$Li_{0.86}Mn_2O_4$" [d]	8.241 [e]	+3.57	+3.55		0.0
b		0.5	"$Li_{0.68}Mn_2O_4$" [d]	8.214 [e]	+3.66	+3.61		0.1
c		1.0	"$Li_{0.36}Mn_2O_4$" [d]	8.067 [e]	+3.82	+3.80		0.0
d		2.0–4.0	"$Li_{0.13}Mn_2O_4$" [d]	8.039 [e]	+3.94	+3.94		0.0
2a	0.05	0.25	"$Li_{0.84}Mn_{1.94}O_4$" [d]	8.237 [e]	+3.69			
b		0.5	"$Li_{0.69}Mn_{1.95}O_4$" [d]	8.201 [e]	+3.75			
c		1.0	"$Li_{0.29}Mn_{1.95}O_4$" [d]	8.055 [e]	+3.95			
d		2.0–4.0	"$Li_{0.18}Mn_{1.92}O_4$" [d]	8.045 [e]	+4.07	+3.97		0.2
3a	0.1	0.25	$Li_{0.85}Mn_{1.90}O_{3.98}$	8.215	+3.74			
b		0.5	$Li_{0.69}Mn_{1.91}O_{3.98}$	8.168	+3.83			
c		1.0	$Li_{0.31}Mn_{1.91}O_{3.98}$	8.067	+4.03		0.1	
d		2.0–4.0	$Li_{0.29}Mn_{1.89}O_{3.98}$	8.061	+4.06	+3.97	0.0	0.1
4a	0.15	0.25	$Li_{0.96}Mn_{1.85}O_{3.95}$	8.204	+3.75			
b		0.5	$Li_{0.76}Mn_{1.85}O_{3.95}$	8.163	+3.86			
c		1.0	$Li_{0.30}Mn_{1.85}O_{3.95}$	8.083	+4.06		0.2	
d		2.0–4.0	$Li_{0.38}Mn_{1.84}O_{3.95}$	8.070	+4.09	+3.99	0.2	0.2
5a	0.2	0.25	$Li_{0.90}Mn_{1.80}O_{3.93}$	8.174	+3.87	+3.76	0.0	0.2
b		0.5	$Li_{0.65}Mn_{1.90}O_{3.93}$	8.154	+4.01	+3.83	0.0	0.3
c		1.0	$Li_{0.33}Mn_{1.80}O_{3.93}$	8.070	+4.18	+3.97	0.0	0.4
d		2.0–4.0	$Li_{0.14}Mn_{1.78}O_{3.93}$	8.048	+4.34	+3.96	0.4	0.7
6a	0.25	0.25	$Li_{0.94}Mn_{1.76}O_{3.91}$	8.155	+3.91	+3.82		0.2
b		0.5	$Li_{0.75}Mn_{1.75}O_{3.91}$	8.136	+4.04	+3.88		0.3
c		1.0	$Li_{0.26}Mn_{1.74}O_{3.91}$	8.093	+4.35	+3.91	0.3	0.8
d		2.0–4.0	$Li_{0.10}Mn_{1.74}O_{3.91}$	8.075	+4.44	+3.94	0.7	0.8
7a	0.3	0.25	$Li_{0.97}Mn_{1.72}O_{3.86}$	8.163	+3.92	+3.81	0.0	0.2
b		0.5	$Li_{0.77}Mn_{1.72}O_{3.86}$	8.127	+4.04	+3.87	0.0	0.3
c		1.0	$Li_{0.29}Mn_{1.70}O_{3.86}$	8.100	+4.37	+3.95	0.4	0.7
d		2.0–4.0	$Li_{0.24}Mn_{1.71}O_{3.86}$	8.075	+4.40	+3.96	0.8	0.7

[a] Correlated with the fixed oxygen content of the corresponding starting spinel.
[b] ±0.003 Å.
[c] Calculated with the Li:Mn:O ratio of the forth column.
[d] Multiphase.
[e] Main phase.
[f] Calculated via the difference between consumed H^+ and H^+ according to Hunter (see text).
[g] Calculated from the difference between Ox_{Mn} calc. and Ox_{Mn} exp. (see text).

of Table 2. Furthermore, the H^+ content can be deduced independently from the difference between the observed and calculated Ox_{Mn} values (ΔOx_{Mn}, nineth column in Table 2). (Note that for the fully extracted products both values are in good agreement.)

From the complete set of experimental data of the extraction products of the system $Li_{1+x-y}Mn_{2-x}O_{4-\delta}$ it follows that the Hunter mechanism is only valid for $x=0$ and mainly for $x=0.05$. However, with increasing x a second mechanism of $Li^+ \leftrightarrow H^+$ exchange gains in importance at the expense of the Hunter model.

3.2.2. ^1H solid state NMR

The incorporation of H^+ in the extraction residues of Li-rich spinels was investigated by ^1H-MAS solid state NMR for several materials. In all cases a signal with a Knight shift around 8 ppm is observed. As example the ^1H-MAS-NMR spectrum of $H_{0.8}Li_{0.24}Mn_{1.71}O_{3.86}$ (sample no. 7d; extraction product from $Li_{1.30}Mn_{1.70}O_{3.86}$; sample no. 7) is shown in Fig. 8. The Knight shift is situated in the typical region for bound protons, whereas the presence of physisorbed H_2O can be excluded.

3.2.3. FT-IR spectroscopic investigations

The results of the IR spectroscopic investigations are summarized for the examples with $x=0$; 0.1 and 0.3 in Fig. 9. Similar to the case of Br_2/CH_3CN extraction (cf. Section 3.1.2), the spectra are characterized in the region of the ν_1 and ν_2/ν_3 of the spinel lattice by two groups of intense vibrations around 650 and 550 cm^{-1}. A comparison of the spectra of the starting spinel and several extraction products

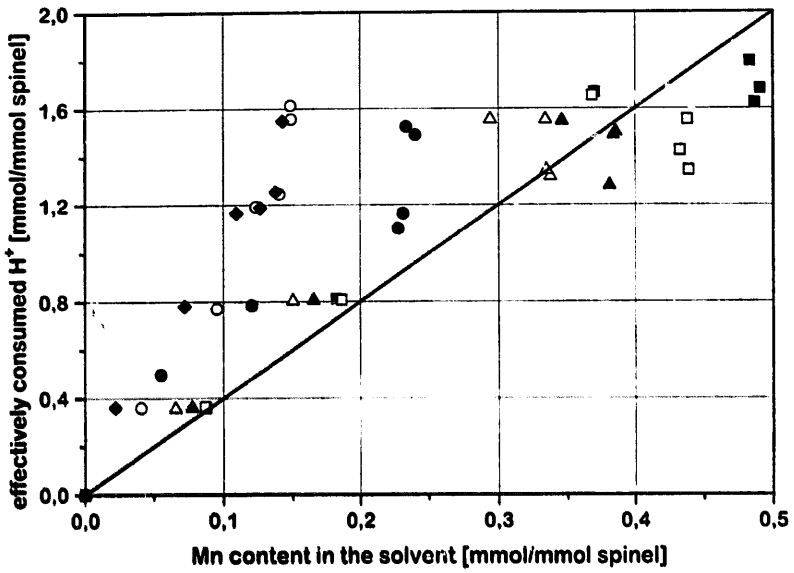

Fig. 7. Dependence of the effectively consumed H^+ vs. Mn concentration in the solvent for H_2SO_4/H_2O extraction of one mole of several members from the spinel system $Li_{1-x}[Li_xMn_{2-x}]O_{4-\delta}$ for: (■) $x=0$; (□) $x=0.05$; (▲) $x=0.1$; (△) $x=0.15$; (●) $x=0.2$; (○) $x=0.25$, and (◆) $x=0.3$. The solid line is the calculated correlation by validity of the Hunter mechanism.

with different H^+:Li$[Li_xMn_{2-x}]O_{4-\delta}$ ratios for the series with $x=0$ indicate the development of a finestructure in the ν_1 and ν_2/ν_3 region with increasing H^+ content in the extraction medium. Interestingly, within the series with $x=0.05$ a very similar behaviour is observed [30], whereas all extraction products from Li-rich spinels with $x \geq 0.1$ do not develop such a pronounced fine structure (e.g. Fig. 9(b)); further examples are shown in Ref. [30]). This means that the appearance of the numerous shoulders in the extraction products is combined with their multiphase nature, visible exclusively for $x=0$ and $x=0.05$ (cf. Section 3.2.4). The occurrence of several spinel phases in the extraction products was explained before by a step-wise extraction of Li^+ from 8*a* (cf. Section 3.1.1 and Refs. [19–21]). Due to the low scattering power of Li no superstructures are observable in XRD, whereas other Li spinels with a clearly detectable order are well known. One example is the 1:3 order spinel $LiNi_{0.5}Mn_{1.5}O_4$ which shows a pronounced fine structure in its IR spectrum. If one disturbs the ordering by increasing substitution the fine structure fades away [31]. Another example is $Li_{0.5}Ga_{2.5}O_4$ and its substitution products [32].

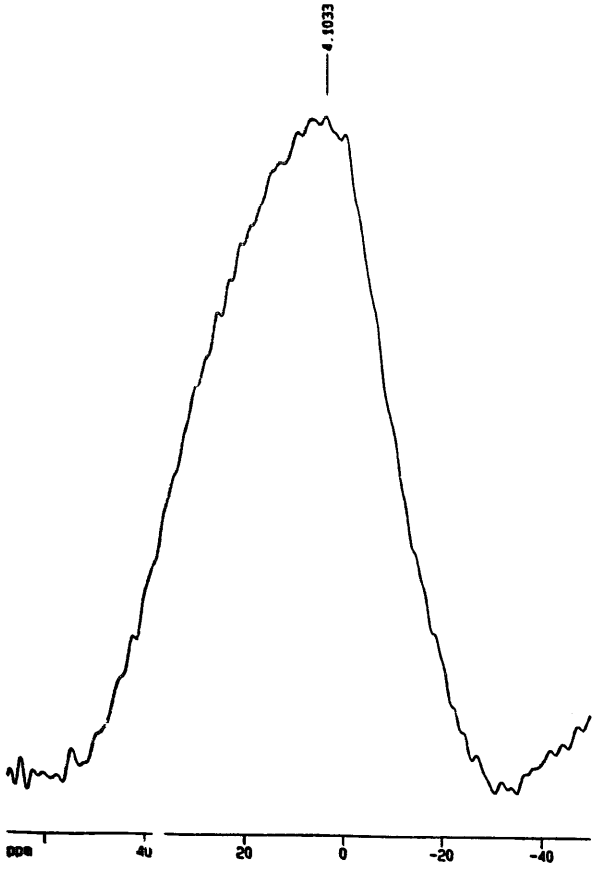

Fig. 8. ^{1}H-MAS-NMR spectrum of the product of Li extraction from the spinel $Li_{1.3}Mn_{1.7}O_{3.86}$ (sample $H_{0.8}Li_{0.24}Mn_{1.71}O_{3.86}$).

Compared with the starting material in the IR spectra of the extraction products from Li-rich spinels with $x \geq 0.1$ only minor changes in the ν_1 and ν_2/ν_3 region are observed (Fig. 9(b) and (c)). However, the presence of H^+ ions due to a $Li^+ \leftrightarrow H^+$ exchange is clearly identified by the appearance of an additional vibration at higher frequencies around 900 cm^{-1}. The assignment is done in analogy with the interpretation of the IR spectrum of protonated electrochemical prepared MnO_2 (EMD) [33]. As one can expect from the data (Table 2) the intensity of this vibration increases with increasing H^+ content. Furthermore, the treatment of fully extracted materials with 0.1 M LiOH solution at RT for 10 h leads to a re-exchange between $H^+ \leftrightarrow Li^+$ and the vibration around 900 cm^{-1} disappears.

3.2.4. Crystal structure

Earlier investigations of the crystal structure within the entire spinel phase $Li_{1+x}Mn_{2-x}O_{4-\delta}$ indicate that the 8*a* positions are exclusively occupied by Li, whereas Li and

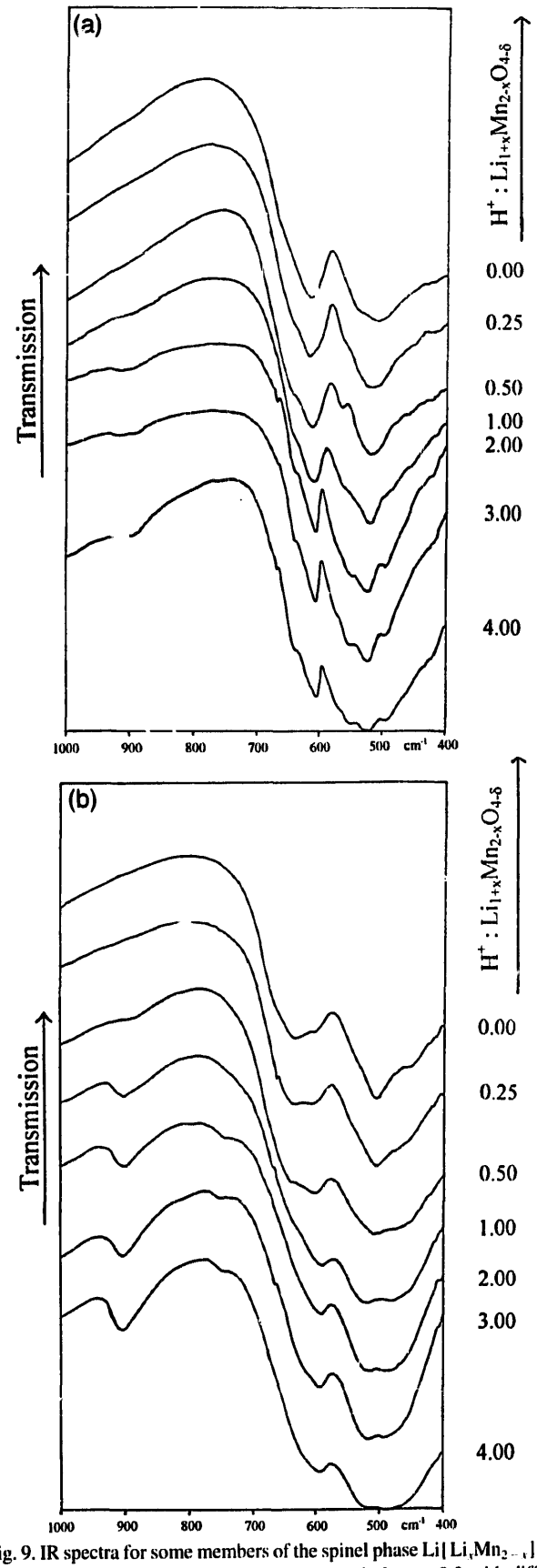

Fig. 9. IR spectra for some members of the spinel phase $Li[Li_xMn_{2-x}]O_{4-\delta}$ and their extraction products for (a) $x=0$, and (b) $x=0.3$ with different ratios of H^+:$Li[Li_xMn_{2-x}]O_{4-\delta}$=0.00 (starting material); 0.25; 0.50; 1.00; 2.00; 3.00 and 4.00. For clarity the spectra are shifted along the y-axis.

Mn reside in 16*d* according to the general formula $Li[Li_xMn_{2-x}]O_{4-\delta}$ [5,6]. In all materials no indications for an exchange between Mn and Li in 8*a* were found. According to Tarascon et al. [34] those spinel compounds are characterized by an additional redox peak at 4.5 V in the cyclic voltammogram.

In Fig. 10 the XRD pattern of the starting spinels are compared to the diagrams of the residues from various H^+:$Li[Li_xMn_{2-x}]O_{4-\delta}$ ratios for $x=0$; and $x=0.1$ (further examples are shown in Ref. [30]). In case of $x=0$ (Fig. 10(a)) the action of the small H^+ fraction of H^+:$LiMn_2O_4$=0.25:1 generates a multiphase material with one prominent cubic spinel phase of slightly reduced lattice constant. Due to the inferior intensity of the reflections from the byproducts no determination of their lattice constants is possible. However, the observation of two satellites (one separate peak and one shoulder) on both sides of the predominant (111) peak indicate the presence of the additional spinel-related phases. Irrespectively of the increasing H^+ concentration in the extraction liquid the materials remain multiphase, but the intensity ratio between the different components varies. Moreover, each group of peaks is shifted to higher diffraction angles, thus indicating a contraction of the crystal framework. Even for high H^+ concentrations of 2.0:1 (border-line value according to the Hunter model) and a significant excess of H^+ of 3.0:1 and 4.0:1 the residue remains multiphase, easily visible by two shoulders in the (111) region and one additional diffraction peak at about $2\vartheta=44°$. Note that Hunter firstly observed this peak in his acid delithiation product of $LiMn_2O_4$ [9]. He explained its appearance by the presence of some starting spinel in the core of the grains. However, this explanation is not convincing since in the region of the likewise intense (311) reflection no satellite is visible around $2\vartheta=35°$. Moreover, we attempted to break of the hypothetical inhomogenity between surface and core of the extracted grains by vigorous grinding. But we obtained no differences in our XRD pattern. So, the different phases are homogeneously distributed within the extraction product of $x=0$. The lattice constant of the most prominent spinel phase is indicated in Table 2.

As in the $x=0$ case extraction products with $x=0.05$ are uniformely multiphase. But smaller variations of the intensity distribution within each group of peaks indicate a shift of the relative quantity of the main phase and the different byproducts. Furthermore, the lattice constant of the main product decreases in comparison with $x=0$ (Table 2). (Note that even for $x=0.05$ the diffraction peak at about $2\vartheta=44°$ is present in the fully extracted products together with two satellites in the (111) region).

In contrast to the cases of $x=0$ and $x=0.05$, the extraction products from materials with $0.1\leq x\leq 0.3$ are uniformely single phase for all ratios between H^+:$Li[Li_xMn_{2-x}]O_{4-\delta}$. As an example Fig. 10(b) shows the XRD patterns for the extraction products with $x=0.1$. All diagrams are typical for single phase cubic spinels of space group $Fd\bar{3}m$. With increas-

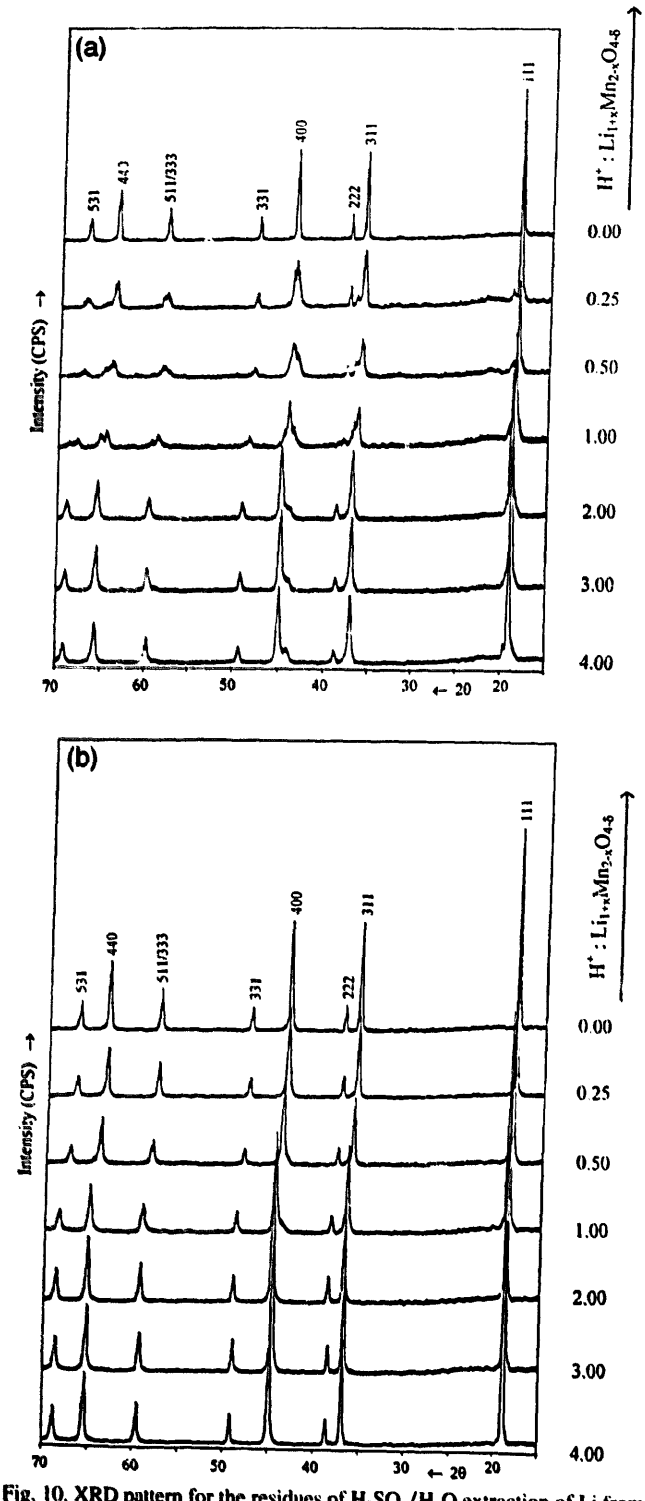

Fig. 10. XRD pattern for the residues of H_2SO_4/H_2O extraction of Li from the spinel system $Li_{1+x}Mn_{2-x}O_{4-\delta}$ for (a) $x=0$, and (b) $x=0.1$ with different values of H^+:$Li[Li_xMn_{2-x}]O_{4-\delta}$ of 0.00 (starting material); 0.25; 0.50; 1.00; 2.00; 3.00 and 4.00. The Miller indices are given for each Bragg peak with reference to the setting of the cubic spinel unit cell ($Fd\bar{3}m$).

ing Li extraction, y, the lattice constant of the spinel phase decreases as indicated in Table 2.

In Fig. 11 the dependence of the spinel lattice constant a from the remaining Li content $(1-y)$ in 8a is summarized for the system $Li_{1-y}[Li_xMn_{2-x}]O_{4-\delta}$. The data indicate, that with decreasing Li content $(1-y)$ the lattice constant firstly decreases steadily (but not linearly). Between $0.2 \leq (1-y) \leq 0.4$ a gap is present, whereas fully extracted materials are uniformly characterized by significantly smaller lattice constants around 8.06 Å. In earlier investigations Pistoia and Wang [35] summarized the results from the literature for the extraction products $Li_{1-y}[Mn_2]O_4$ from the spinel $Li[Mn_2]O_4$. The authors observed a gap for $0.3 \leq (1-y) \leq 0.6$ and explained this finding on the basis of the electrochemical studies of Ohzuku et al. [19] by a two-step extraction mechanism. This model postulated in the first step a single phase oxidation with a continuous lattice contraction from $a=8.239(3)$ to 8.142(2) Å [19]. The second step is described by a two-phase equilibrium between two cubic phases with $a \approx 8.14$ Å and $a=8.045(6)$ Å [19].

According to our combined results from H_2SO_4/H_2O and Br_2/CH_3CN extractions of spinels from the entire system $Li[Li_xMn_{2-x}]O_{4-\delta}$ multiphase residues are observed exclusively for $x=0$ and $x=0.05$ whereas Li-rich extraction products with $0.1 \leq x \leq 1/3$ are uniformly single phase. Thus, the two-step mechanism can only be applied for $x=0$ and $x=0.05$. However, even in these cases our results are in contradiction with the results from the literature, because materials with $(1-y) \leq 0.6$ are invariably multiphase, due to ordering effects in 8a. It is very likely, that Li ordering is also responsible for the gap in Fig. 11, because certain Li:□ ratios in 8a will be more suitable for cationic ordering than others. Accordingly, extraction products with unsuitable Li contents are unstable.

Due to our quantitative studies, the validity of the Hunter mechanism is confined to $x=0$ (with $x=0.05$ as a borderline case). For $x \geq 0.1$ additional extraction modes must be working. One possibility for the explanation of the high Li extraction level in Li-rich spinels is the assumption of a disproportion of Mn^{4+} into Mn^{2+} and higher valent Mn species. For example an acidic extraction mechanism for $Li[Li_{1/3}Mn_{5/3}]O_4$ is given by the following relation

$$Li[Li_{1/3}Mn_{5/3}]O_4 + 8/3H^+ \rightarrow 2/3MnO_4^- + Mn^{2+} + 4/3Li^+ + 4/3H_2O$$

Indeed, Li extraction with half concentrated H_2SO_4 results in the formation of an extraction residue together with MnO_4^-, easily detectable by its violet color. However, this model does not explain the presence of H^+ in our fully extracted residues (Table 2). Furthermore, no MnO_4^- is detected in the extraction liquid for H^+:$Li_{1+x}Mn_{2-x}O_{4-\delta} \leq 4.0$.

On the other hand, a satisfying agreement with the experimental results is obtained for an ion exchange $Li^+ \leftrightarrow H^+$. This mechanism was postulated before in case of $LiMn_2O_4$ by several authors. However, only small quantities of H^+ were detected analytically [10,36–40]. These findings are confirmed by our own results for $x=0$, whereas with increasing Li content the $Li^+ \leftrightarrow H^+$ exchange mechanism gains in importance and the Hunter mechanism is suppressed.

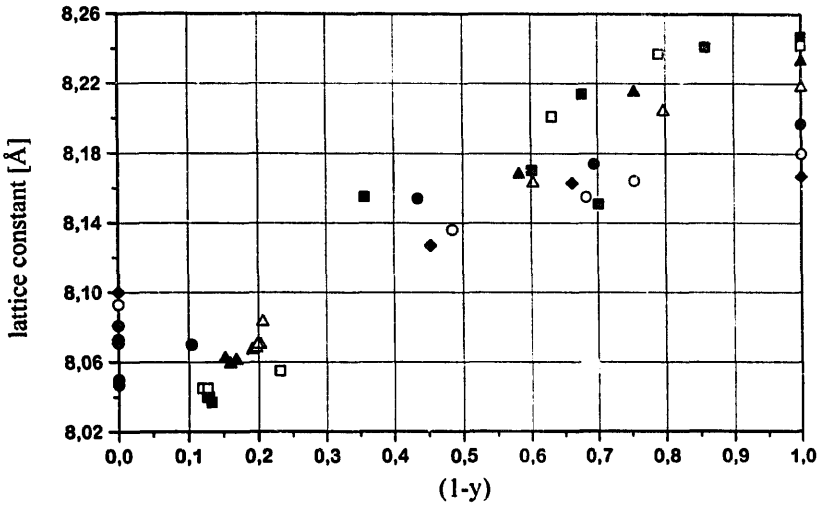

Fig. 11. Lattice constant vs. Li content in 8*a* of the residue $(1-y)$ for some members of the spinel phase $Li[Li_xMn_{2-x}]O_{4-\delta}$ and their extraction products $Li_{1-y}[Li_xMn_{2-x}]O_{4-\delta}$ for: (■) $x=0$; (□) $x=0.05$; (▲) $x=0.1$; (△) $x=0.15$; (●) $x=0.2$; (○) $x=0.25$, and (◆) $x=0.3$. For the residues with $x=0$ and $x=0.05$ the lattice constant of the main phase is indicated.

4. Conclusions

The behaviour of Li extraction in the entire system $Li_{1-y}[Li_xMn_{2-x}]O_{4-\delta}$ is not uniform. According to our present results of chemical Li extraction and the electrochemical data [6], the system can be subdivided into three regions:

(i) In region I with $0 \leq x < 0.05$ the spinel framework is not stable against Li extraction, due to the large volume decrease of about 7.5% between the starting material and the fully extracted spinel. The extraction products are always multiphase due to a tendency of ordering between Li and □ in 8*a*. The electrochemical performance in region I is unsatisfying [6].

(ii) In region II ($0.05 < x \leq 0.2$) the spinel framework is stable against Li extraction. The extraction products of the different extraction levels are uniformely single phase. The total volume decrease between starting spinel and fully extracted material decreases to about 5.5% ($x=0.1$) and 4.5% ($x=0.2$). All materials are slightly oxygen deficient. The best cathode materials for rechargeable Li^+ batteries are situated in this region around $x=0.1$.

(iii) In region III ($0.2 \leq x \leq 0.33$) the host matrix is again stable against Li extraction. All materials are oxygen deficient. So, even spinels with $x=0.33$ conserve a minor ability for Li extraction. However, the observed capacity is too low for practical applications in the 4 V region. Moreover, materials of the region III show a strong tendency for an ion exchange $Li^+ \leftrightarrow H^+$ and may lose additional lithium via traces of water in the extraction liquid.

Acknowledgements

This work was supported by the 'Bundesministerium für Bildung, Wissenschaft, Forschung und Technologie' as well as by the 'Verband der Chemischen Industrie'. We are indepted to Mrs A. Ehmann and Mrs E. Niquet for their helpful assistance.

References

[1] K. Mizushima, P.C. Jones, P.J. Wiseman and J.B. Goodenough, *Mater. Res. Bull., 15* (1980) 783.
[2] M.M. Thackeray, W.I.F. David, P.G. Bruce and J.B. Goodenough, *Mater. Res. Bull., 18* (1983) 461.
[3] M.M. Thackeray, P. Johnson, L.A. de Picciotto, P. Bruce and J.B. Goodenough, *Mater. Res. Bull., 19* (1984) 179.
[4] R.J. Gummov, A. de Kock and M.M. Thackeray, *J. Solid State Chem., 69* (1994) 59.
[5] P. Endres, B. Fuchs, S. Kemmler-Sack, K. Brandt, G. Faust-Becker and H.-W. Praas, *Solid State Ionics, 89* (1996) 221, and Refs. cited therein.
[6] S. Kemmler-Sack, B. Fuchs, P. Endres, H.-W. Praas and K. Brandt, in F. Beck (ed.), *GdCH-Monographie, Vol. 3, Elektrochemie der Elektronenleiter*, 1996, p. 342.
[7] A. Yamada, *J. Solid State Chem., 122* (1996) 160.
[8] B. Fuchs, *Diplomarbeit*, University of Tübingen, 1990.
[9] J.C. Hunter, *J. Solid State Chem., 39* (1981) 142.
[10] J.B. Goodenough, M.M. Thackeray, W.I.F. David and P.G. Bruce, *Rev. Chim. Miner., 21* (1984) 435.
[11] J.C. Hunter and F.B. Tudron, in B. Schumm (ed.), *Proc. Symp. Manganese Dioxide Electrode, Theory and Practice, Pennington, NJ, USA, 1985*, p. 444.
[12] A. Moshbah, A. Verbaiere and M. Tournoux, *Mater. Res. Bull., 18* (1983) 1375.
[13] V. Manev, A. Monchilov and A. Nassalevska, *J. Power Sources, 43* (1993) 551.
[14] M.M. Thackeray, S.D. Baker, R.T. Adendorff and J.B. Goodenough, *Solid State Ionics, 17* (1985) 171.
[15] W.I.F. David, M.M. Thackeray, L.A. de Picciotto and J.B. Goodenough, *J. Solid State Chem., 67* (1987) 316.
[16] A. Ott, *Diplomarbeit*, University of Tübingen, 1996.
[17] G. Blasse, *J. Inorg. Nucl. Chem., 25* (1963) 743.
[18] B. Krutzsch and S. Kemmler-Sack, *Mater. Res. Bull., 18* (1983) 647.
[19] T. Ohzuku, M. Kitagawa and T. Hirai, *J. Electrochem. Soc., 137* (1990) 769.
[20] Y. Xia and M. Yoshio, *J. Electrochem. Soc., 143* (1996) 825.

[21] W.I.F. David, M.M. Thackeray, L.A. de Picciotto and J.B. Goodenough, *J. Solid State Chem.*, *67* (1987) 316.
[22] A.R. Wizansky, P.E. Ranch and F.J. Disalvo, *J. Solid State Chem.*, *81* (1989) 203.
[23] N. Kumagai, T. Fujiwara, K. Tanno and T. Horiba, *J. Electrochem. Soc.*, *143* (1996) 1007, and Refs. cited therein.
[24] Y. Kanzaki, A. Tamiguchi and M. Abe, *J. Electrochem. Soc.*, *138* (1991) 333.
[25] C. Ryter, *Phys. Rev. Lett.*, *5* (1960) 10.
[26] L. Schutte, G. Colsmann and B. Reuter, *J. Solid State Chem.*, *27* (1979) 227.
[27] P. Tarte and J. Preudhomme, *Spectrochim. Acta*, *A26A* (1970) 747.
[28] J. Preudhomme and P. Tarte, *Spectrochim. Acta*, *A27A* (1971) 1817.
[29] J. Preudhomme and P. Tarte, *Spectrochim. Acta*, *A28* (1972) 60.
[30] P.L. Endres, *Ph.D. Thesis*, University of Tübingen, 1996.
[31] G. Gryffroy and R.E. Vandenberghe, *J. Phys. Chem. Solids*, *53* (1992) 777.
[32] F. Hochu, M. Lenglet and C.K. Jorgensen, *J. Solid State Chem.*, *120* (1995) 244.
[33] F. Fillaux, H. Ouboumour, C.H. Cachet, J. Tomkinson, C. Levy Clement and L.T. Yu, *J. Electrochem. Soc.*, *140* (1993) 592.
[34] J.M. Tarascon, W.R. McKinnon, F. Coowar, T.N. Bowmer, G. Amatucci and D. Gyomard, *J. Electrochem. Soc.*, *141* (1994) 1421.
[35] G. Pistoia and G. Wang, *Solid State Ionics*, *66* (1993) 135.
[36] G.V. Leont'eva, *Russ. J. Inorg. Chem.*, *33* (1988) 1254.
[37] M.M. Thackeray and A. de Kock, *J. Solid State Chem.*, *74* (1988) 414.
[38] M.H. Roussow, D.C. Liles and M.M. Thackeray, *J. Solid State Chem.*, *104* (1993) 464.
[39] J.R. Dahn, E.W. Fuller, M. Obravac and U. van Sacken, *J. Solid State Ionics*, *69* (1994) 265.
[40] J. Morales, R. Stoyanova, J.L. Tirado and E. Zhecheva, *J. Solid State Chem.*, *113* (1994) 184.